Geoscience Frontiers 10 (2019) 1359–1370

HOSTED BY

Contents lists available at ScienceDirect

China University of Geosciences (Beijing)

Geoscience Frontiers

journal homepage: www.elsevier.com/locate/gsf

Research Paper

A new cache of Eoarchaean detrital zircons from the Singhbhum craton, eastern India and constraints on early Earth geodynamics

Bulusu Sreenivas [a,*], Sukanta Dey [b], Y.J. Bhaskar Rao [a], T. Vijaya Kumar [a], E.V.S.S.K. Babu [a], Ian S. Williams [c]

[a] CSIR-National Geophysical Research Institute, Hyderabad 500007, India
[b] Department of Earth Sciences, Indian Institute of Science Education and Research, Kolkata 741246, India
[c] Research School of Earth Sciences, The Australian National University, Canberra 2601, Australia

ARTICLE INFO

Article history:
Received 29 November 2018
Received in revised form
24 January 2019
Accepted 5 February 2019
Available online 15 March 2019
Handling Editor: M. Santosh

Keywords:
U–Pb zircon ages
Hf isotopes
Singhbhum craton
Hadean
Eoarchean
Geodynamics

ABSTRACT

The dominant geodynamic processes that underpin the formation and evolution of Earth's early crust remain enigmatic calling for new information from less studied ancient cratonic nuclei. Here, we present U–Pb ages and Hf isotopic compositions of detrital zircon grains from ~2.9 Ga old quartzites and magmatic zircon from a 3.505 Ga old dacite from the Iron Ore Group of the Singhbhum craton, eastern India. The detrital zircon grains range in age between 3.95 Ga and 2.91 Ga. Together with the recently reported Hadean, Eoarchean xenocrystic (up to 4.24 Ga) and modern detritus zircon grains from the Singhbhum craton, our results suggest that the Eoarchean detrital zircons represent crust generated by recycling of Hadean felsic crust formed at ~4.3–4.2 Ga and ~3.95 Ga. We observe a prominent shift in Hf isotope compositions at ~3.6–3.5 Ga towards super-chondritic values, which signify an increased role for depleted mantle and the relevance of plate tectonics. The Paleo-, Mesoarchean zircon Hf isotopic record in the craton indicates crust generation involving the role of both depleted and enriched mantle sources. We infer a short-lived suprasubduction setting around ~3.6–3.5 Ga followed by mantle plume activity during the Paleo-, Mesoarchean crust formation in the Singhbhum craton. The Singhbhum craton provides an additional repository for Earth's oldest materials.

1. Introduction

The dominant geodynamic processes in the early Earth and the evolution of the crust-mantle systems through the Hadean and Archean Eons continue to be enigmatic (Harrison et al., 2008, 2017; Kemp et al., 2010, 2015; Bell et al., 2014; Zeh et al., 2014; Hawkesworth et al., 2017; Mueller and Nutman, 2017). The rock record pertaining to these periods being scarce, much of the information on early crust formation and crust-mantle interactions is derived largely from the detrital zircon grains entrained in younger rocks (Harrison et al., 2008, 2017; Hawkesworth et al., 2017; Mueller and Nutman, 2017). The best studied ancient detrital zircon grains are from the Jack Hills metaconglomerate/quartzite, Yilgarn craton, Western Australia (Wilde et al., 2001; Harrison et al., 2008; Kemp et al., 2010). Together with constraints from numerical models, the U–Pb age and Hf isotope data of these ancient zircon grains have led to disparate views on the nature of early crust and geodynamic processes (Harrison et al., 2008; Korenaga, 2013; O'Neill and Debaille, 2014; Gerya et al., 2015; Nutman et al., 2015; Hawkesworth et al., 2017). The interpretations regarding composition of the Hadean crust vary from dominantly mafic to that with significant felsic components and the inferred geodynamic models include subduction plate tectonics, stagnant lid, heat pipe and plume tectonics (Nutman et al., 2015; Hawkesworth et al., 2017; Mueller and Nutman, 2017). Beginning with the Eoarchean, the zircon Hf isotope record of both magmatic and sedimentary rocks shows evidence for short-lived juvenile magmatic events defined by chondritic Hf isotope compositions as early as 4.1–3.85 Ga ago (Harrison et al., 2008; Wu et al., 2008; Næraa et al., 2012; Bell et al., 2014). This has been interpreted as evidence for an increased role of the depleted mantle reservoir, indicating a shift in the geodynamic regime towards plate tectonic-like scenarios (Harrison et al., 2008; Nutman et al., 2013), although the timing of this purported shift is

* Corresponding author.
E-mail address: bsreenivas@ngri.res.in (B. Sreenivas).
Peer-review under responsibility of China University of Geosciences (Beijing).

https://doi.org/10.1016/j.gsf.2019.02.001

equivocal (Harrison et al., 2008; Kemp et al., 2010; Nutman et al., 2015; Hawkesworth et al., 2017). The post-3.0 Ga record of zircon U–Pb ages of the continental crust is marked by prominent peaks and troughs that correlate with periods of supercontinent assembly and breakup (Belousova et al., 2010; Condie and Aster, 2010; Voice et al., 2011; Roberts and Spencer, 2015; Iizuka et al., 2017). However, an extension of this interpretation into the Eo- to Paleoarchean interval (pre-3.2 Ga) remains controversial (Nutman et al., 2013; Hawkesworth et al., 2017). Further, the available record for this time window appears to vary among the different cratons. The process of juvenile crust formation and crustal recycling in the Phanerozoic and Proterozoic orogenic systems is consistent with the plate tectonics paradigm, where zircon age–Hf isotope composition distributions manifest as distinct arrays (Collins et al., 2011; Spencer et al., 2013; Roberts and Spencer, 2015). Since ~550 Ma, the range of ε_{Hf} values narrows towards super-chondritic values in the accretionary (external) orogens as against a broadening trend for the collisional (internal) orogens (Collins et al., 2011).

The discovery and characterization of ancient zircon grains from different cratons, each with a geological record attesting to the diversity of tectonic settings, assumes importance in understanding the spatio-temoporal variations. Here we report new zircon U–Pb age and Hf isotope data spanning nearly a billion years between 3.95 Ga and 2.91 Ga from the Singhbhum craton, eastern India. Together with the recent reports of Hadean and Eoarchean ages for xenocrystic zircon from a sample of Paleoarchean gneiss (Chaudhuri et al., 2018), TTG suites (Dey et al., 2017) and detrital zircon grains from modern river sediments (Miller et al., 2018), we discuss here major Hadean and Archean crust formation events in the Singhbhum craton.

2. Geological setting of the Singhbhum craton

The peninsular Indian shield is an ensemble of crustal terranes that include Archean (>2.5 Ga) cratonic nuclei such as the Singhbhum, Bastar, Dharwar and Bundelkhand-Aravalli cratons with a pervasive Meso- to Neoarchean and rare Paleoarchean rock record (Naqvi, 2005; Ramakrishnan and Vaidyanathan, 2008; Sarkar and Gupta, 2012). The Singhbhum craton (Fig. 1) in the eastern part of the Indian shield is a well-studied Archean granite greenstone terrane. It is among the oldest of the Archean cratonic nuclei that comprise the Indian shield (Mukhopadhyay et al., 2008; Dey et al., 2017; Chaudhuri et al., 2018; Miller et al., 2018). The Singhbhum craton, an elliptical Archean low metamorphic grade granite-greenstone terrane, is bound by the Phanerozoic Damodar Valley and Mahanadi Valley grabens to the north and southwest and the Proterozoic Eastern Ghats Granulite Terrane to the southeast. The northern and southern limits comprise prominent thrust zones (Sarkar and Saha, 1983; Saha et al., 1988; Mukhopadhyay, 2001; Roy and Bhattacharya, 2012). The Archean basement of this low-medium grade (greenschist-amphibolite facies) metamorphic terrane comprises ~3.53–3.29 Ga tonalite-trondhjemite-granodiorite (TTG) gneisses referred to as the Older Metamorphic Tonalite Gneiss (OMTG) and over a dozen granitoid plutons collectively known as Singhbhum Granite (SG) (Dey et al., 2017) with supracrustal rock enclaves, the Older Metamorphic Group (OMG). The central granite-gneiss domain is surrounded by belts of 3.5–3.4 Ga supracrustal rock successions (greenstones), the Iron Ore Group (IOG).

2.1. The granitoids (OMTG, SG and OMG suites)

The recent U–Pb zircon age data on the Singhbhum craton have been summarized by Dey et al. (2017) and shown in Fig. 2. The central part of the craton comprises OMTG, SG and OMG rock suites. The age of magmatism has been constrained at about 3.47 Ga, 3.35 Ga and final phase at 3.30 Ga (Dey et al., 2017). Their geochemical characteristics suggest crustal reworking caused by episodic plume in an oceanic plateau with no involvement of mantle (Dey et al., 2017).

2.2. The supracrustals (Iron Ore Group)

The most widespread Archean supracrustal successions of the craton comprise the Iron Ore Group (IOG), shallow and deep water facies sedimentary rock units such as Banded Iron Formation (BIF), quartzites, metapelites and carbonates interlayered with mafic and felsic metavolcanic rocks (Mukhopadhyay et al., 2008). The IOG is one of the best preserved Paleoarchean greenstone successions known in the Indian shield. It is distributed in three synformal discontinuous basins referred to here as the eastern (the Gorumahisini–Badampahar basin), western (the Koira-Jamda basin) and southern (the Tomka-Daitari basin)-IOG. These successions consist of low metamorphic grade rock units including bimodal (mafic/ultramafic and felsic) metavolcanics, pillowed and/or massive metabasalt with subordinate felsic lava-tuff, minor units of bedded chert, shale and a prominent Banded Iron Formation – BIF (Mukhopadhyay et al., 2008). The volcanic suite is tholeiitic with rare komatiite. The greenstone sequence in the southern IOG (S-IOG) is in thrust contact with the Paleo- to Mesoarchean Sukinda ultramafic rocks that are inter-layered with podiform chromitites (Mondal et al., 2007; Mukhopadhyay et al., 2008). Based on the lithological association, structure and geochemical signatures both plume-related (Prabhakar and Bhattacharya, 2013; Dey et al., 2017) and plate tectonic-style (Mukhopadhyay et al., 2008, 2012) models have been advocated for this granite-greenstone terrane. The S-IOG belt and the enclosing Singhbhum granites are overlain unconformably by detached belts of thick shelf-facies mature quartzites, conglomerates, and mud stones (about 1500 m thick) with minor volcanics (Mukhopadhyay et al., 2014; Ghosh et al., 2016) collectively referred to here as the Mahagiri quartzites (Fig. 3). A generalized stratigraphic succession of the S-IOG is given in Fig. 4. The present study is centered on S-IOG, where a deep-marine depositional setting based on extensive development of pillowed and massive mafic lavas interbedded with bedded chert, felsic lava units and BIFs (up to 120 m thick) has been described (Mukhopadhyay et al., 2008; Ghosh et al., 2016). The dacitic volcanic unit has been described as a deep-water facies ash-poor, non-vesiculated, welded pyroclastic units erupted under a steam cupola. The volcanic succession progressively aggraded to a shallow water facies followed by the deposition of BIFs. Trace element data show enrichment of La/Nb, Th/Nb, Th/La, Ba/La, Pb/Ce and depletion in Nb–Ta relative to neighboring REEs comparable to volcanic rocks from the Phanerozoic suprasubduction arc-forearc settings (Mukhopadhyay et al., 2012). The Mahagiri quartzites are deposited on the SG granites representing the final phase of sedimentation during the Archean period of the Singhbhum craton. A paleosol is reported at the basement cover interface (Mukhopadhyay et al., 2014). In this study, detrital zircon grains from two samples of Mahagiri quartzite (IOG-6 and SC-17-7) and zircon separates from a dacite lava sample (SC-17-2) from the S-IOG (Fig. 3) have been analyzed for U–Pb and Hf isotope compositions.

3. Methods and materials

The zircon analyses were performed using Sensitive High Resolution Ion Microprobe (SHRIMP), Laser Ablation (LA) Inductively Coupled Plasma Mass Spectrometer (ICP-MS) and multi collector (MC) ICP-MS techniques.

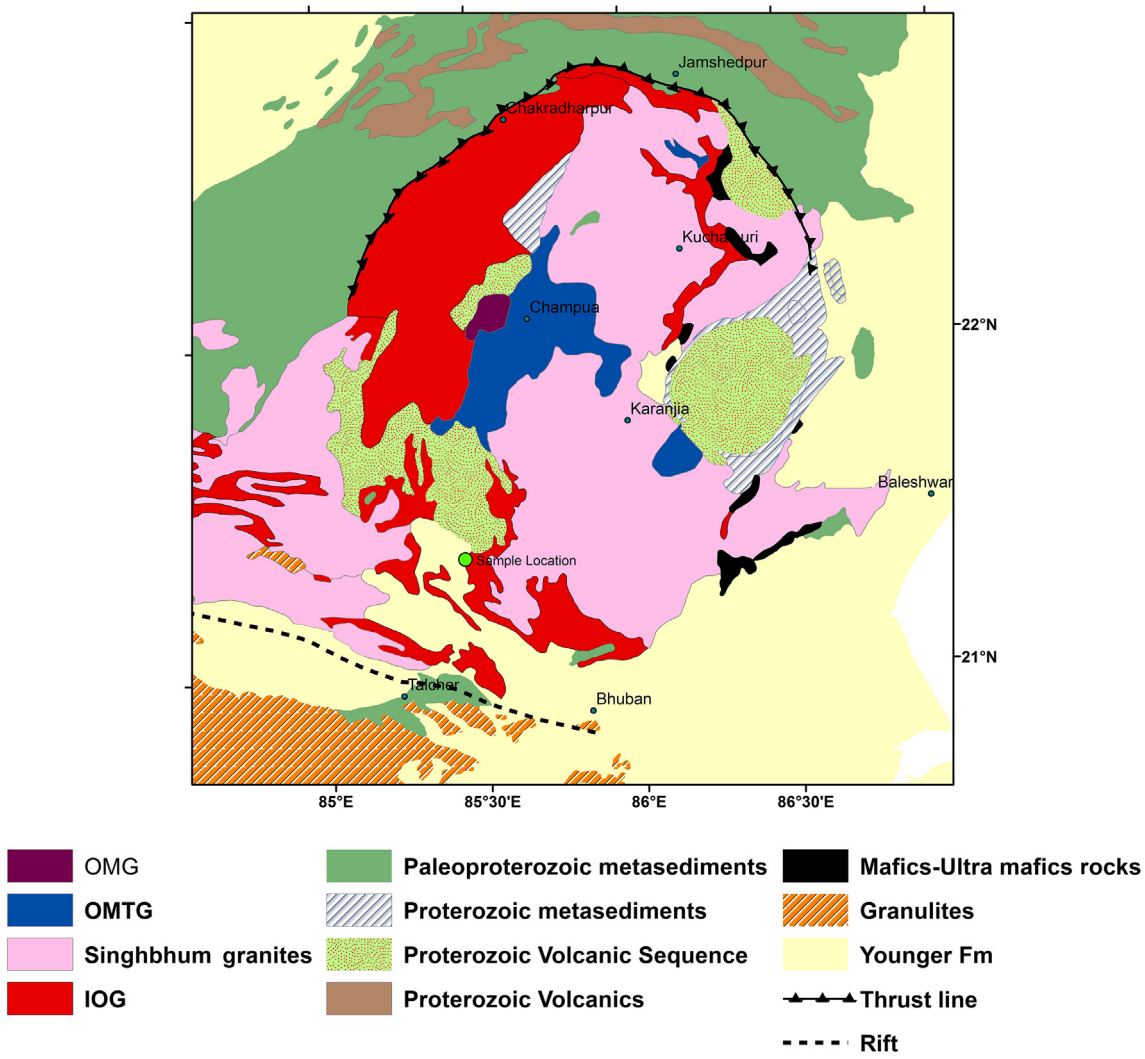

Figure 1. Simplified geology of the Archean Singhbhum Craton (SC). OMG: Older Metamorphic Group; OMTG: Older Metamorphic Tonalite Gneiss; IOG: Iron Ore Group.

The zircon grains were separated by clean heavy-mineral separation techniques and mounted in epoxy resin. The detrital zircon grains were first analyzed using a 213 nm New Wave Nd-YAG LA system coupled to a quadrupole ICP-MS at Council of Scientific Industrial Research-National Geophysical Research Institute (CSIR-NGRI), revealing the extreme antiquity of some grains. Aliquots of zircon from the same quartzite and dacite samples were analyzed for U–Pb isotopes using the SHRIMP IIe at Geoscience Australia (GA). All Hf isotope measurements were carried out using a Resolution 193 nm EXCIMER LA coupled to MC-ICP-MS (Nu-HR) at CSIR-NGRI. The laser spots for Hf isotope analysis coincided with those of SHRIMP analyses.

Sample IOG-6 was processed for zircon extraction at Indian Institute of Technology (Indian School Mines), Dhanbad. Samples SC-17-2 and SC-17-7 were processed at CSIR-NGRI. A random fraction of zircon separates from sample IOG-6 was analyzed for U–Pb by LA-ICP-MS at CSIR-NGRI and another fraction of zircon from the same sample, and those from the two other samples, were analyzed by SHRIMP IIe at GA.

3.1. U–Pb analysis by LA-ICP-MS

A detailed account of the analytical procedure, instrument conditions and data processing is given in Appendix I and summarized briefly below. Samples were crushed, milled and sieved for ~300 μm to 50 μm grain size. Zircon concentrates were obtained by a combination of Wilfley shake table, Franz isodynamic magnetic separator, methylene iodide heavy liquid and handpicked under a binocular microscope. Zircon grains were mounted in epoxy resin discs, polished, carbon coated and CL images were obtained using VEGA3 TESCAN SEM-CL at the CSIR-NGRI. These were imaged at a working distance of 17 mm and accelerating voltage of 15–20 kV. Zircon U–Pb dating was performed using a 213 nm Nd-YAG (UP213, New Wave Research) LA system coupled to Thermo Xseries^{II} ICP-MS. The isotopic analyses followed standard zircon bracketing using zircon standard GEMOC-GJ1, additionally zircon standards OGC, 91500 as well as TEMORA were analyzed as unknowns in each session for monitoring reproducibility and instrument stability. The laser spot size was 40 μm with a typical pit depth of 30–50 μm, with 10 Hz repetition rate and fluence around 12 mJ/cm^2. Each ablation comprised measurement of blank for 60 s followed by data acquisition up to 120 s for masses ^{204}Pb, ^{206}Pb, ^{207}Pb, ^{208}Pb, ^{232}Th, ^{235}U and ^{238}U as explained elsewhere (Griffin et al., 2004; Babu et al., 2009). Common Pb corrections were performed by Andersen's method (Andersen, 2002) because of the extremely low ^{204}Pb and a potential interference from ^{204}Hg. The software package GLITTER was used offline for calculating the U–Pb ages

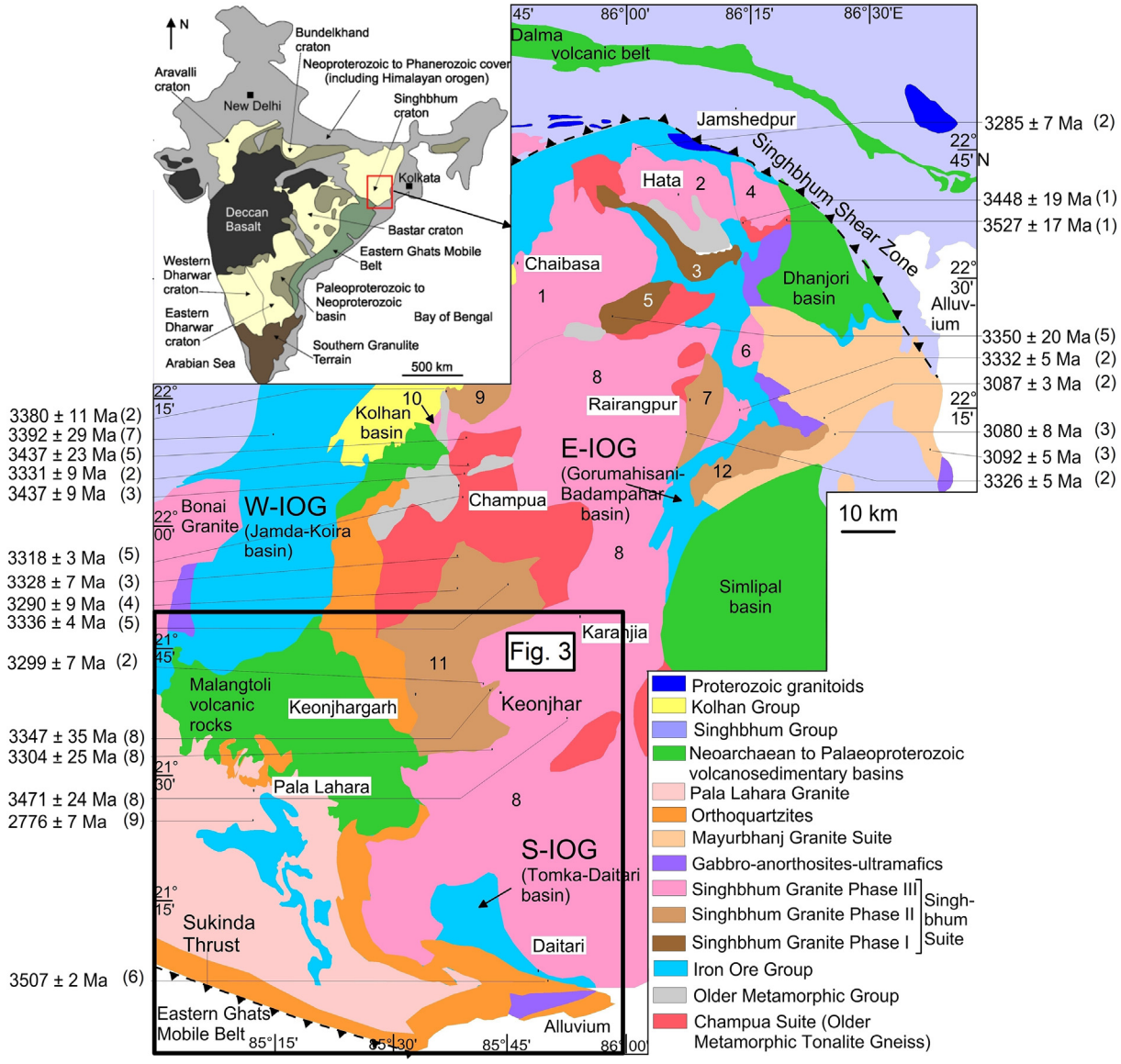

Figure 2. Geological map of the Singhbhum craton (modified after Dey et al., 2017) showing the location of Fig. 3, the S-IOG. Sources for the zircon U–Pb ages are referred in parenthesis: (1) Acharyya et al. (2010); (2) Nelson et al. (2014); (3) Misra et al. (1999); (4) Tait et al. (2011); (5) Upadhyay et al. (2014); (6) Mukhopadhyay et al. (2008); (7) Basu et al. (2008); (8) Dey et al. (2017); (9) Chattopadhyay et al. (2015).

from the raw signal data. Isoplot version 3.0 (Ludwig, 2003) was used for U–Pb concordia plots. $^{206}Pb/^{238}U$ vs. $^{207}Pb/^{235}U$ age for zircon standard GJ1 during this study was 615 ± 15 Ma (2σ, MSWD = 0.1, n = 10) and that for OGC was 3408 ± 100 Ma (2σ, MSWD = 1.3, n = 9) and 91500 was 1068 ± 27 Ma (2σ, MSWD = 2.2, n = 4). These values are consistent with the published LA-ICP-MS age data for the stated standards (Andersen, 2002; Jackson et al., 2004; Stern et al., 2009).

3.2. U–Th–Pb analysis by SHRIMP IIe

The zircon was prepared for SHRIMP analysis by casting several hundred grains in an epoxy mount with zircon standards TEMORA 2 and SL13. The grains were exposed by hand on 1200 grade SiC paper, then polished mechanically using 3 and 1 μm diamond paste. After CL imaging on a JEOL JSM-6610 SEM at the Research School of Earth Sciences, ANU, the mounts were thoroughly cleaned in petroleum benzine, RBS detergent solution and Millipore water, then coated with 13 nm of high purity Au.

The zircon grains were analyzed for U–Th–Pb isotopes on the SHRIMP IIe ion microprobe at GA using a procedure based on that described in Williams and Claesson (1987), Claoué-Long et al. (1995) and Williams (1998). In brief, the zircon grains were sampled with a ~3 nA, 10 kV, negative O_2 primary ion beam focused to a spot 20 μm diameter. Positive secondary ions sputtered from the zircon were extracted at 10 kV and analyzed at a mass resolution of ca. 5000 by peak stepping through the Zr, Pb, U and Th isotopes of interest, using a single ETP discrete-dynode electron multiplier and magnet field switching. Each analysis consisted of 4 cycles through the isotope sequence, taking ~9 min.

U–Th–Pb ratios were determined with reference to TEMORA 2 (radiogenic $^{206}Pb/^{238}U$ = 0.06683) and U concentrations with reference to SL13 (238 ppm U). Pb isotopic compositions were measured directly without correction for instrumental mass fractionation (<1‰ / amu). The data were reduced using in-house

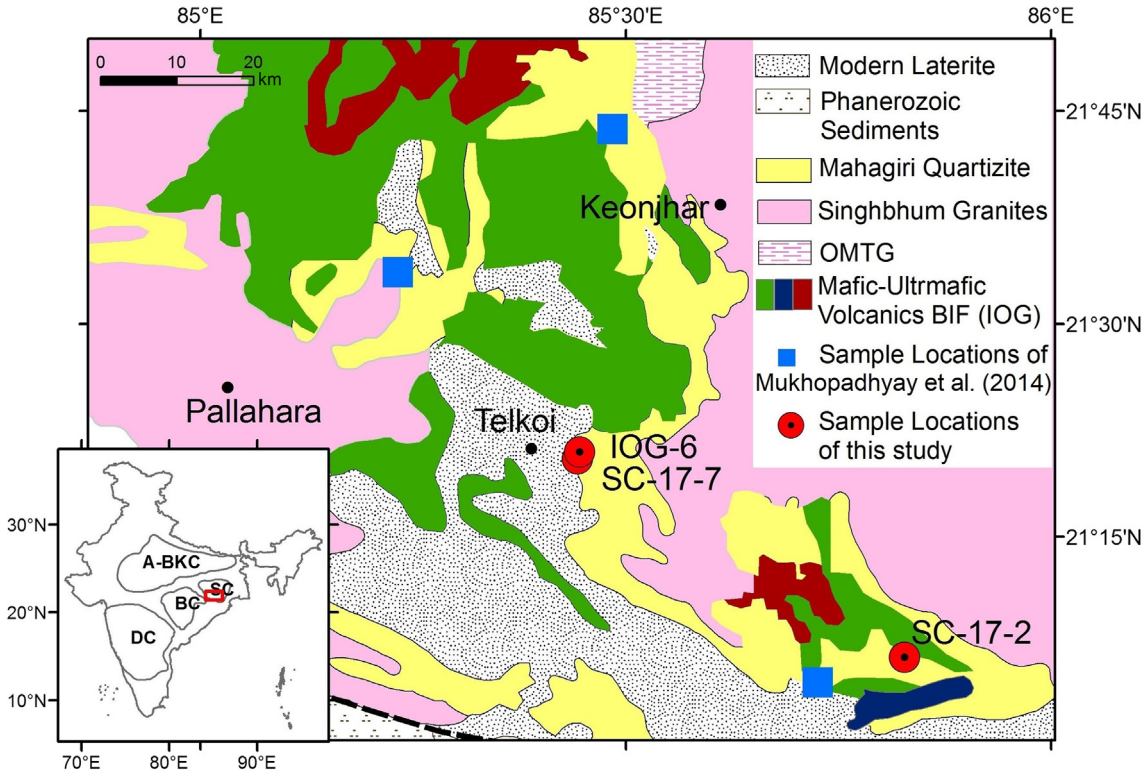

Figure 3. Geological map of parts of southern and western IOG showing location of quartzite samples.

PRAWN and LEAD software. All analyses were corrected for common Pb using the measured ^{204}Pb and a common Pb composition corresponding to the age of the analyzed spot (Cumming and Richards, 1975). Uncertainties in the date of an individual spot mentioned in the text, listed in data tables and plotted on the concordia diagrams are ± 1σ.

3.3. Lu–Hf isotopic analysis by LA-MC-ICP-MS

A Resolution SE 193 nm ArF Excimer laser ablation system with a Laurin Technic S155 dual-volume laser ablation cell connected to a Nu Plasma high-resolution MC-ICP-MS was used for the Lu, Hf, Yb isotopic measurements at CSIR-NGRI. Zircon grains with ≤10% discordant SHRIMP U–Pb spot ages were analyzed by placing laser spots right on those of SHRIMP. The Nu Plasma analytical procedure is similar to those given in (Griffin et al., 2006; Vijaya Kumar et al., 2017). Time-resolved analyses using Nu Plasma software were performed with the laser-ablation system operating at 10 Hz frequency, 38 μm spot size, and 80% energy with fluence 12 J/cm^2. Background was measured for 60 s, while the duration of data acquisition varied between 90 s and 120 s. Standard zircon GJ1 was the internal standard and analyzed repeatedly in cycles each bracketing 5 unknown zircon grains accompanied with standard TEMORA and Mud Tank for monitoring data quality and reproducibility. Interferences of ^{176}Lu and ^{176}Yb on ^{176}Hf were corrected using measured intensities of interference-free ^{175}Lu and ^{172}Yb (Griffin et al., 2004, 2006). Initial ^{176}Hf/^{177}Hf ratio at the age of the zircon spot was calculated using the decay constant of 1.865 × 10^{-11} yr^{-1} (Scherer et al., 2001) the measured ^{176}Hf/^{177}Hf ratio, and the inferred zircon crystallization age from the U–Pb concordia. Epsilon Hf (ε_{Hf}) values were calculated with reference to the chondrite reservoir (CHUR) assuming present-day chondritic ^{176}Hf/^{177}Hf and ^{176}Lu/^{177}Hf values of 0.282772 ± 0.000029 and 0.0332 ± 0.0002, respectively (Blichert-Toft and Albarède, 1997). Calculated depleted-mantle model ages (T_{DM}) based on the measured ^{176}Lu/^{177}Hf ratios represent minimum crustal residence ages tend to be not reliable for unradiogenic Hf isotope compositions. Hence, a two-stage model age was calculated using the measured ^{176}Lu/^{177}Hf value of each spot at the age of the zircon (T_{DM}, first stage), a ^{176}Lu/^{177}Hf of 0.015 (Griffin et al., 2000) for the average continental crust (T_{DM}^{C}, second stage), and depleted-mantle ^{176}Lu/^{177}Hf and ^{176}Hf/^{177}Hf values of 0.0384 (Scherer et al., 2001) and 0.283251 (Nowell et al., 1998). During the analytical sessions the Geostandards GJ1, Temora2 and 91500 zircon standards were also repeatedly measured, for which normalized ^{176}Hf/^{177}Hf values and weighted averages are 0.282005, ε_{Hf} = 13.51 ± 0.72 (n = 10); 0.282742, ε_{Hf} = 8.4 ± 1.3 (n = 10); 0.282432, ε_{Hf} = 11.6 ± 1.5 (n = 5), respectively, where uncertainties are 1σ deviations. These values are indistinguishable, within limits of error, from the laser-ablation MC-ICP-MS measurements at elsewhere for the two standards (Griffin et al., 2007; Clements et al., 2012).

4. Results

4.1. Zircon textures and U, Th abundance

The detrital zircon grains are typically 50–120 μm in length except for a few fragments of larger grains. The aspect ratios are typically 1:2 and rarely 1:3. The zircon grains vary in shape from elliptical to nearly rounded indicating significant sedimentary transportation prior to the deposition of Mahagiri sandstones. The Cathodoluminescence (CL) images for a few representative zircon grains from the samples IOG-6 and SC-17-7 are shown in Fig. 5a–c, where most images represent longitudinal cross-sections. In general, these zircon grains are characterized by low to moderate luminescence and commonly show oscillatory growth zoning.

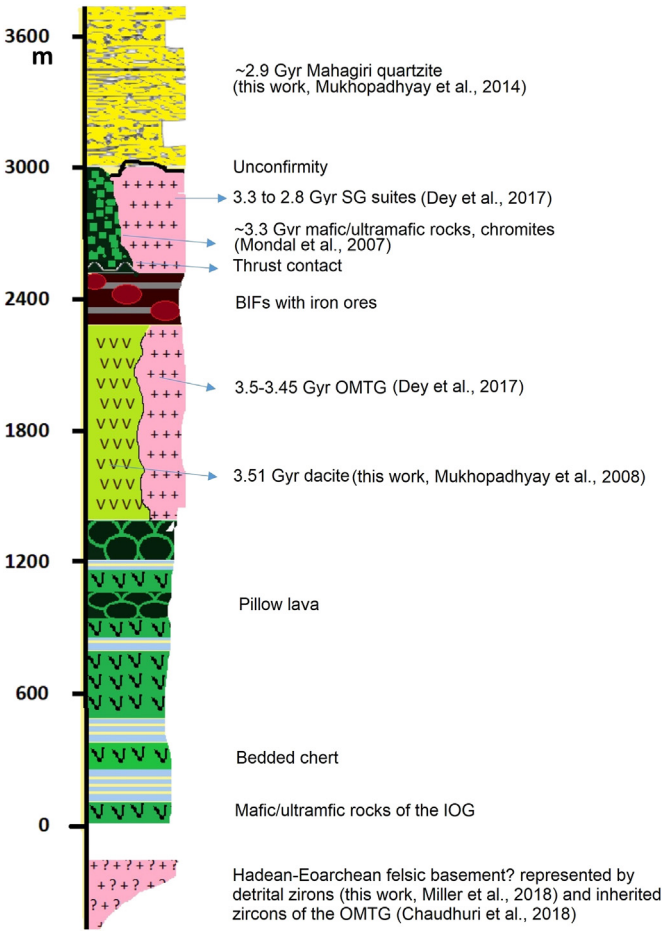

Figure 4. A generalized stratigraphic succession of S-IOG.

Some grains show sector zoning (e.g., grain Nos. IOG-6-2-39, 36, 37, in Fig. 5a; IOG-6-27, 68 in Fig. 5b). Patchy zoning is rare. Apart from dark metamictic domains in a few grains, no fluid or mineral inclusions are discernible. These textures suggest preservation of primary magmatic character of a vast majority of the zircon grains analyzed here. However, a few grains have thin (<5 μm) discontinuous brightly luminescent rims (e.g., IOG-6-39 and IOG-6-2-39, Fig. 5a), which may represent relict metamorphic zircon overgrowths. Apart from these, most of the zircon grains lack metamorphic overgrowths. Effects of alteration indicated by bright luminescent patches across growth zoning and/or metamictization is common to many grains, such domains were avoided in the analysis and analytical spots were placed in crack and inclusion-free domains showing uniform luminescence. In sample IOG-6, more than two-thirds of the analyzed zircon grains are concordant (≤10% discordance). The concordant zircon grains have U content between 12 ppm and 451 ppm (avg. 145 ppm), Th ranging between 8 ppm and 314 ppm (avg. 90 ppm) and the Th/U values lie between 0.17 and 1.79 (avg. 0.70). In most cases, the discordant zircon grains have a similar range of U, Th and Th/U values but some have clearly higher abundance of U (up to 723 ppm), Th (up to 1023 ppm) and Th/U (up to 2.12).

In sample SC-17-7, nearly all zircon grains are concordant with U abundance ranging between 41 ppm and 566 ppm (avg. 179 ppm), Th ranges between 11 ppm and 627 ppm (avg. 318 ppm) and the Th/U between 0.12 and 1.70 (avg. 0.66). The Th/U values (consistently >0.1) of the detrital zircon grains from the Mahagiri quartzites are comparable with values reported for igneous zircon in several studies elsewhere (e.g., Rubatto, 2002; Cavosie et al., 2004). The reason(s) for the higher U, Th and Th/U values in the discordant zircon grains is ambiguous, but may be related to effects of metamictization as indeed evident from the CL images of the grains with higher values.

Zircon grains from the sample SC-17-2, dacitic lava are in the 50–100 μm range, generally preserving prism and pyramidal outlines and a clear concentric (oscillatory) growth zoning typical of magmatic zircon. These zircon grains have U concentrations ranging between 65 ppm and 280 ppm (avg. 162 ppm), and Th between 42 ppm and 370 ppm (avg. 165 ppm). Th/U values range between 0.59 and 1.40 (avg. 0.93). The microtextures and Th/U values indicate typical magmatic character.

4.2. Zircon U–Pb ages

The U–Pb age and Hf isotope compositions of the analyzed zircon grains from the three samples are given as supplementary data table (Appendix II) and represented as concordia plots in Fig. 6. The $^{207}Pb/^{206}Pb$ age spectra of detrital zircon grains with U–Pb isotopic compositions that are ≤10% discordant are shown in Fig. 7. SHRIMP U–Pb age data of sample IOG-6 yielded 6 zircon grains with Eoarchean ages between 3950 Ma and 3661 Ma, along with a dominant (86%) Paleo- to Mesoarchean population (3510–3176 Ma) (Fig. 7a). Additionally, LA-ICP-MS analysis indicates 6 Eoarchean zircon grains with ages between 3947 Ma and 3601 Ma from the sample IOG-6 (Fig. 7a). These data show continuous spread of ages between 3.95 Ga and 3.6 Ga. On the other hand, a gap in the zircon age data between 4.0 Ga and 3.7 Ga is evident in recently published data (Chaudhuri et al., 2018; Miller et al., 2018). Notably, our data fills in this gap resulting in a contiguous Hadean–Eoarchaen spread of zircon ages from the Singhbhum craton. The Eoarchean source rocks for these sediments are unknown/inaccessible. The age spectra of detrital zircon population from sample SC-17-7 and seven other quartzite samples from the region reported earlier (Mukhopadhyay et al., 2014) are shown in Fig. 7b. The crystallization ages of these range from 3580 Ma to 2909 Ma. The dominant age population (57% in sample SC-17-7; Fig. 7b) range between 3220 Ma and 3438 Ma, with a prominent peak at ~3.35 Ga. The age spectra of zircon from modern river sands from the craton (Miller et al., 2018) as well as the Archean sandstones (Mukhopadhyay et al., 2014) show a similar range and prominent peak at ~ 3.35 Ga. This, along with the smaller peaks (<10%) at ~3.5 Ga and ~3.1 Ga, correlates with available U–Pb zircon age data from the OMTG, SG and felsic volcanic suites (Fig. 2). The age limit to the deposition of Mahagiri quartzites was constrained previously at 3.02 Ga (Mukhopadhyay et al., 2014). However, zircon spot ages between 2909 Ma and 2970 Ma from sample SC-17-7 (3 grains), may constrain deposition of the Mahagiri quartzite to be younger than 2909 Ma. Although this population of <3.0 Ga zircon grains is statistically insignificant (<5%), the fact that the 2909 Ma zircon is concordant supports our inference. The Eoarchean zircon grains are found only in sample IOG-6, probably localized in a specific stratigraphic unit, analogous to the restricted occurrence of abundant >4.0 Ga zircon population in the Jack Hills metasedimentary belt (Wilde et al., 2001). The zircon crystals from a dacitic lava from the S-IOG yield a concordant U–Pb age of 3505.5 ± 5.0 Ma, with MSWD = 0.64 (Fig. 8), which is indistinguishable from an earlier report of 3506.8 ± 2.3 Ma (Mukhopadhyay et al., 2008), confirming its precise age and the view that the S-IOG is the oldest greenstone sequence in the Indian shield.

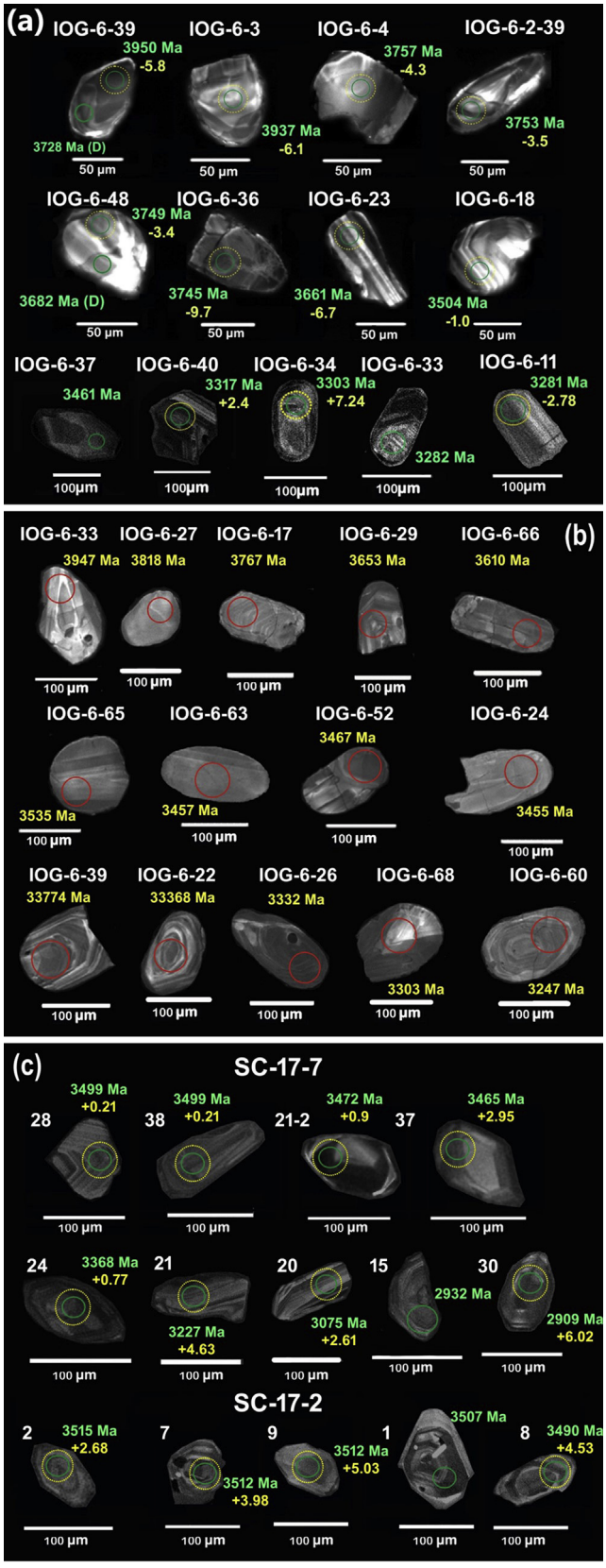

Figure 5. CL images of representative zircons of this study. The spot ages in Ma and $\varepsilon_{Hf}(t)$ values are shown. SHRIMP spot – green circle; LA-MC-ICP-MS spot – yellow circle. (a) CL images of zircon grains of sample IOG-6 analyzed by SHRIMP, (b) analyzed by LA-ICP-MS and (c) zircon grains of samples SC-17-7 and SC-17-2 analyzed by SHRIMP.

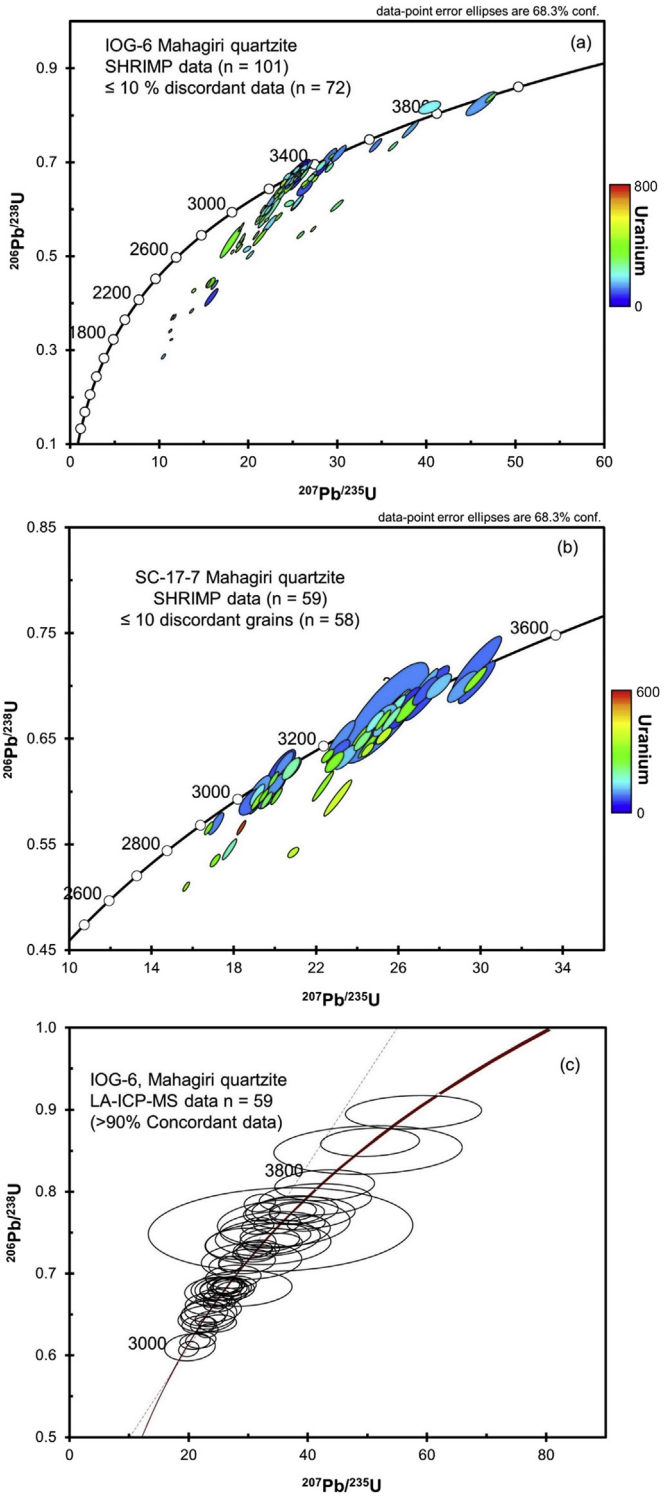

Figure 6. U–Pb concordia diagrams of (a) zircons of sample IOG-6 and (b) sample SC-17-7 analyzed using SHRIMP and (c) LA-ICP-MS analysis of zircons of sample IOG-6.

4.3. Zircon Hf isotope compositions

Fig. 9a shows a plot of zircon Hafnium isotope compositions and age for the two quartzite samples and one dacite along with published data on both magmatic (from OMTG and SG, Dey et al., 2017; Chaudhuri et al., 2018) and detrital zircon grains from modern river

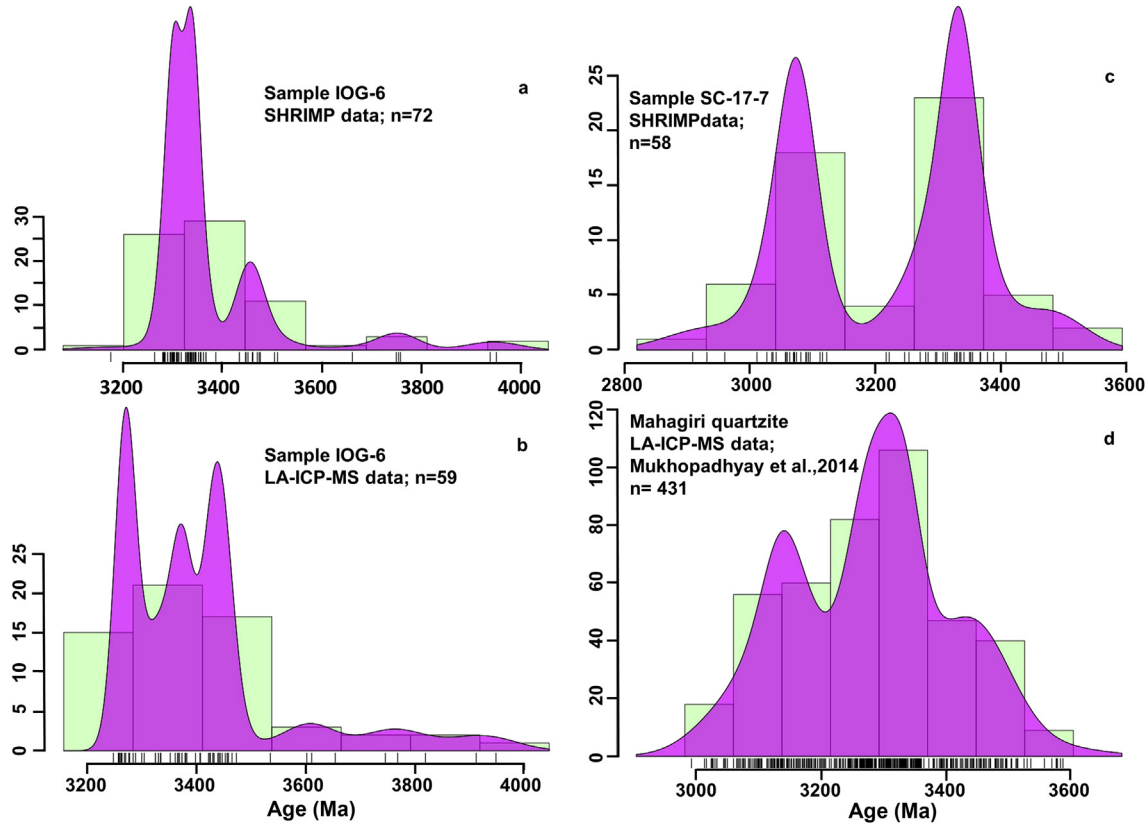

Figure 7. Kernel Density Estimate plots (using ISOPLOTR; Vermeesch, 2018) of $^{207}Pb/^{206}Pb$ age spectra of detrital zircons from Mahagiri quartzites. (a) Sample IOG-6, SHRIMP data, (b) sample IOG-6, LA-ICP-MS data, (c) sample SC-17-7, SHRIMP data and (d) data from zircon grains of 7 samples of Mahagiri quartzite (Mukhopadhyay et al., 2014), LA-ICP-MS data.

sediment (Miller et al., 2018) of the Singhbhum craton. The Eoarchean detrital zircon grains from sample IOG-6 have markedly unradiogenic Hf isotope compositions ($\varepsilon_{Hf}(t) = -9.7$ to -3.4). The Hadean and Eoarchean xenocrystic and modern detrital zircon analysis also show unradiogenic $\varepsilon_{Hf}(t)$ values (Chaudhuri et al., 2018; Miller et al., 2018). In contrast, the Paleoarchean Singhbhum zircon Hf compositions (this study; Dey et al., 2017; Chaudhuri et al., 2018; Miller et al., 2018) are overwhelmingly radiogenic or super-chondritic. The zircon grains from the 3.51 Ga dacite from the S-IOG have strikingly positive $\varepsilon_{Hf}(t)$ ranging from +0.5 to +7.8, mostly plotting close to the DM curve.

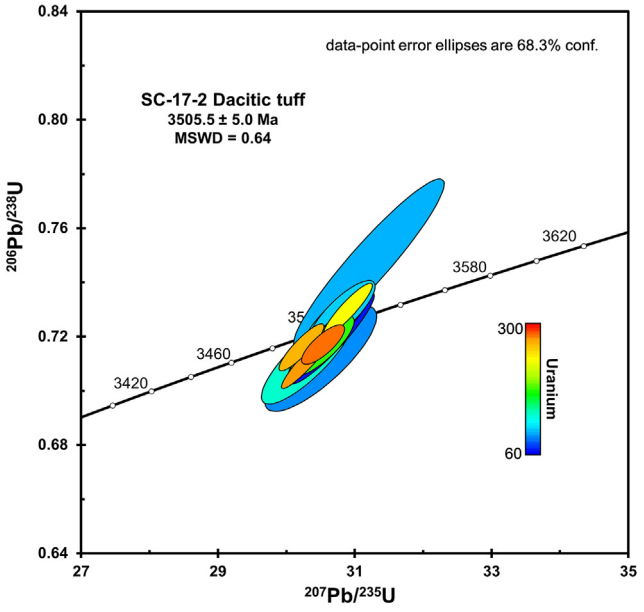

Figure 8. U–Pb concordia plot of zircons from dacite sample (SC-17-2). Symbol colors correspond to U concentration of zircons.

5. Discussion

In general, potential scenarios to explain shifts in $\varepsilon_{Hf}(t)$ from unradiogenic to radiogenic values include: (i) subduction-like processes involving destruction of older crust and addition of new crust (Næraa et al., 2012; Nutman et al., 2013; Bell et al., 2014) and (ii) major mantle overturn events that may lead to establishment of thick mafic plateau (Griffin et al., 2014). However, as stated earlier the timing of subduction initiation has been contentious with proposals ranging from Hadean to Neoarchean. Some authors have proposed that modern style subduction on Earth did not begin until Neoproterozoic (e.g. Stern, 2005; Brown, 2008). Globally, the convergence of several lines of evidence such as the hot asthenosphere, lower rigidity of lithosphere, change in the composition of the juvenile crust, rate of production and destruction of continental crust and recycling of water etc., have been proposed to suggest establishment of plate tectonics ~3.0 Ga (Dhuime et al., 2012; Tang et al., 2016; Hawkesworth et al., 2017). Alternative proposals for the formation of ancient continental masses and rifting around 3.66 Ga and 3.53 Ga, respectively have been suggested (Korenaga, 2013).

A comparison of the Singhbhum data with those from several Archean cratons is presented in Fig. 9b. At the Hadean–Eoarchean transition, several gneissic suites (e.g., Acasta, Itsaq and Anshan) show near chondritic $\varepsilon_{Hf}(t)$ values (Kemp et al., 2015). This suggests

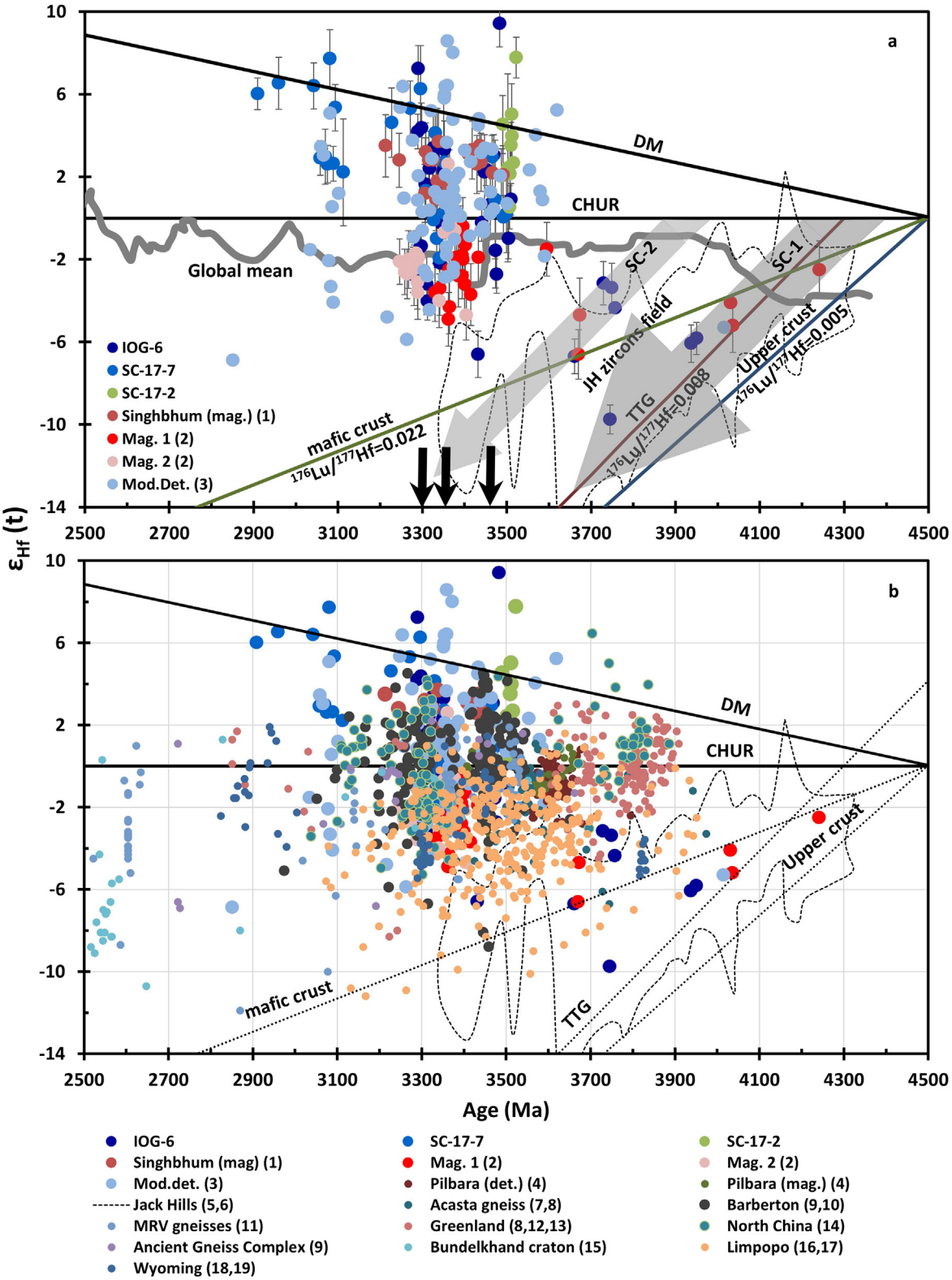

Figure 9. (a) The age vs. $\varepsilon_{Hf}(t)$ ($\varepsilon_{Hf} = ((^{176}Hf/^{177}Hf_{sample})/(^{176}Hf/^{177}Hf_{chondrite}) - 1) \times 10^4$) plot of magmatic and detrital zircons from the Singhbhum craton (data from this work and Dey et al., 2017; Chaudhuri et al., 2018; Miller et al., 2018). CHUR–chondritic uniform reservoir, DM–depleted mantle, JH–Jack Hills zircons (Kemp et al., 2010; Bell et al., 2014). The global mean curve is from Roberts and Spencer (2015). Note a prominent shift in the $\varepsilon_{Hf}(t)$ values at ~3500 Ma in the Singhbhum zircon data and three distinct events of crust generation during the Paleoarchean (thick black arrows on *x*-axis). The unradiogenic $\varepsilon_{Hf}(t)$ values of the Hadean and Eoarchean zircons suggest involvement of mafic protocrust and/or TTG-like sources extracted between ~4200 Ma (SC-1) and 4000 Ma (SC-2). (b) Comparison of the Singhbhum magmatic and detrital zircons with global data (n = 1371). The references to each data set is given in parentheses: (1) Dey et al. (2017); (2) Chaudhuri et al. (2018); (3) Miller et al. (2018); (4) Kemp et al. (2015); (5) Kemp et al. (2010); (6) Bell et al. (2014) (the Jack Hills zircon field in both Fig. 9a, b are drawn after the compilation on the zircons on which coupled Hf–Pb are provided); (7) Iizuka et al. (2009); (8) Amelin et al. (2000); (9) Zeh et al. (2013); (10) Zeh et al. (2011); (11) Satkoski et al. (2013); (12) Næraa et al. (2012); (13) Hiess et al. (2009); (14) Wu et al. (2008); (15) Kaur et al. (2014); (16) Zeh et al. (2010); (17) Zeh et al. (2014); (18) Frost et al. (2017); (19) Mueller and Wooden (2012).

limited or no involvement of Hadean crustal sources in the generation of most Eoarchean felsic crustal components (Kemp et al., 2015). Unlike most Eoarchean gneisses, the 3.95–3.66 Ga Singhbhum detrital zircon populations (this study) as well as the other reported Hadean and Eoarchean zircon data from the craton (Chaudhuri et al., 2018; Miller et al., 2018) suggest involvement of Hadean crust in the generation of their parental melts. On the $\varepsilon_{Hf}(t)$ vs. age plot (Fig. 9a), broad trajectories SC-1 and SC-2 best fit the distribution Singhbhum Hadean–Eoarchean zircon compositions. These trajectories with $^{176}Lu/^{177}Hf = 0.008$ correspond to TTG-like sources that formed at ~4.3–4.2 Ga (SC-1, zircon grains with >3.7 Ga ages) and ~3.95 Ga (SC-2, zircon grains with <3.6 Ga) each followed by a by a continuously decreasing $\varepsilon_{Hf}(t)$ trend. Such a continuous involvement of enriched reservoirs between ~4.2 Ga and 3.6 Ga is inconsistent with magma generation through plate tectonic processes.

The positive $\varepsilon_{Hf}(t)$ values of zircon from the dacite and a vast majority of Paleo-, Mesoarchean detrital population from samples IOG-6 and SC-17-7 have super-chondritic $\varepsilon_{Hf}(t)$. The Paleoarchean magmatic zircon population from the OMTG, SG suites (Dey et al., 2017; Chaudhuri et al., 2018) and those from the modern detritus (Miller et al., 2018) show a wider range including several sub-chondritic $\varepsilon_{Hf}(t)$ values. Overall, the Singhbhum zircon data record a prominent shift from unradiogenic to radiogenic Hf isotope compositions at about 3.6–3.5 Ga. This suggests the establishment of depleted mantle by ~3.5 Ga and its continuous involvement in the Paleo-Measoarchean magmatism of the craton. Though zircon record of several igneous suites of ~4.0 Ga to 3.8 Ga are characterized by positive $\varepsilon_{Hf}(t)$ as stated earlier (see Kemp et al., 2015), recent work on the unaltered igneous rocks from Greenland suggest derivation from chondritic like sources by low volume melting of (Fisher and Vervoort, 2018). This implies that major mantle depleting events might have occurred between 3.6 Ga and 3.5 Ga globally. The overall Eoarchean age-Hf distribution in the Singhbhum craton is similar to that observed in cratons such as Wyoming, which also record a drastic shift in $\varepsilon_{Hf}(t)$ values at 3.6–3.5 Ga (Mueller and Wooden, 2012). The predominance of radiogenic $\varepsilon_{Hf}(t)$ values in the post-3.5 Ga zircon data from the Singhbhum craton attests to a sustained role of magmatism from depleted mantle sources throughout the Paleo- and Mesoarchean periods. The range of sub-chondritic $\varepsilon_{Hf}(t)$ values of this zircon population suggests involvement of older felsic crust but no older than 3.6 Ga. This implies isolation of the Hadean, Eoarchean crustal sources in the Paleo-, Mesoarchean crust forming events.

Thus it is likely that the Paleo- to Mesoarchean magmatism in the Singhbhum craton involved operation of some form of plate tectonics. Interestingly, a suprasubduction zone setting for the origin of 3.51 Ga bimodal volcanic suite of the S-IOG was proposed based on the geochemical compositions of volcanic rocks (Mukhopadhyay et al., 2012), which is also consistent with our inference of a depleted mantle source for the dacite lava. On the other hand, autochthonous tectonic models involving melting at the base of a thickened oceanic plateau possibly affected by recurrent mantle plumes have been suggested for the TTG components of the craton (Prabhakar and Bhattacharya, 2013; Dey et al., 2017).

In this context, the role of within plate magmatism and vertical tectonics invoked for the classical Palaeo-Mesoarchaean dome and basin greenstone-gneiss terranes (e.g. Singhbhum craton, Prabhakar and Bhattacharya, 2013; Pilbara craton, South Africa, Sandiford et al., 2004; Hawkesworth et al., 2017) assumes significance. In these terrains the generation of TTG components is ascribed to processes such as melting of the base of thickened hydrated basaltic crust (oceanic plataeux; Smithies et al., 2009; Johnson et al., 2017) and/or subduction of the latter (Martin et al., 2014). We suggest here that the 3.51 Gyr bimodal volcanic succession recording strongly positive $\varepsilon_{Hf}(t)$ values of the IOG might represent an early stage of formation of an oceanic plateau possibly in a suprasubduction setting (Mukhopadhyay et al., 2012) related to a short-lived subduction tectonic regime. Further, the presence of both positive and negative $\varepsilon_{Hf}(t)$ values of 3.5–3.2 Ga magmatic and detrital zircon from the craton suggest recurrent mantle upwelling and melting at the base of a progressively thickening oceanic plateau (see also Prabhakar and Bhattacharya, 2013; Dey et al., 2017) similar to Pilbara tectonic model (Smithies et al., 2009; Johnson et al., 2017). This possibly involved cyclic gravitational overturns (Wiemer et al., 2018). This mode of concurrent juvenile felsic and mafic crust generation with associated delamination of residual mafic crust could characterize the pre-plate tectonic scenario prior to 3.2–3.0 Ga period (Hawkesworth et al., 2017) that may correspond to 'lid breaking' event (Beall et al., 2018). We, thus propose that a combination of plate and plume tectonic processes accounts for the Paleo-, Mesoarchaen crust formation in the craton.

In the pre-3.0 Ga period, several Paleo- to Mesoarchean zircon populations from the terranes such as the Limpopo belt (Zeh et al., 2014), Minnesota River Valley gneisses (Satkoski et al., 2013) and Greenland (Næraa et al., 2012), show predominantly unradiogenic $\varepsilon_{Hf}(t)$ values. Their distribution can be explained in terms of recycling of predominantly Eo- to Paleoarchean crustal components. On the other hand, positive $\varepsilon_{Hf}(t)$ values appear starting from ~3.5 Ga in the Singhbhum and North China (Wu et al., 2008; Wan et al., 2015) cratons as well as the Barberton region (Zeh et al., 2013) suggesting addition of voluminous felsic crust generated through processes involving depleted mantle sources. Overall, Paleo- to Mesoarchean terranes record evidence for both simultaneous recycling of older crust and addition of new crust extracted from depleted mantle source in the time period between 3.5 Ga and 3.0 Ga. Interestingly, the recent work on Ti isotope compositions ($\delta^{49}Ti$) in marine shales reflect predominance of felsic crustal components in the provenance since at least ~3.5 Ga, a scenario consistent with operation of plate tectonics by this time (Greber et al., 2017).

6. Conclusions

The zircon age spectra from the Singhbhum craton comprising a continuum from ~4.2 Ga to 2.9 Ga serve as a new repository to understand the early Earth evolution. The detrital zircon U–Pb ages in the Mahagiri quartzite, Singhbhum craton, range from 3.95 Ga to 2.91 Ga and magmatic zircon grains from a dacite sample yield an age of 3505.5 ± 5.0 Ma. Together with recent age–Hf data, the Hadean to Eoarchean zircon populations of the Singhbhum craton indicate recycling of Hadean felsic crust. There is evidence for a drastic shift from unradiogenic to radiogenic Hf isotope compositions at ~3.5 Ga, which continued till 3.0 Ga reflecting a shift in geodynamic regime at the beginning of the Paleoarchean period.

Acknowledgements

We acknowledge Dr. V. M. Tiwari, Director, CSIR-NGRI for encouragement. Financial support from the Ministry of Earth Sciences, New Delhi for Excimer 193 nm LA system at CSIR-NGRI MoES/P.O.(Seismo)/1(245)/2014 and for the project on Singhbhum craton to S. D., E. V. S. S. K. B., B. S. and T. V. K (No. MoES/P.O.(Geosci)45/2015; GAP-738-28EVB). This work forms part of the CSIR-NGRI projects INDEX (PSC0204) and GEOMET. Support from Australian Scientific Instruments and Geoscience Australia in providing access to the SHRIMP IIe, and The ANU for SEM imaging, is acknowledged. Y. J. B. thanks the DAE-Raja Ramanna Fellowship.

Appendix A. Supplementary data

Supplementary data to this article can be found online at https://doi.org/10.1016/j.gsf.2019.02.001.

References

Acharyya, S.K., Gupta, A., Orihashi, Y., 2010. New U-Pb zircon ages from Paleo-Mesoarchean TTG gneisses of the Singhbhum craton, eastern India. Geochemical Journal 44, 81–88.

Amelin, Y., Lee, D.-C., Halliday, A.N., 2000. Early-middle Achaean crustal evolution deduced from Lu–Hf and U–Pb isotopic studies of single zircon grains. Geochimica et Cosmochimica Acta 64, 4205–4225.

Andersen, T., 2002. Correction of common Pb in U–Pb analyses that do not report ^{204}Pb. Chemical Geology 192, 59–79.

Babu, E.V.S.S.K., Bhaskar Rao, Y.J., Vijaya Kumar, T., 2009. In: Aggarwal, S.K., et al. (Eds.), In-situ U-Pb and Hf-Isotopic Characterization of GJ-1 Zircon by Laser Ablation ICP-MS and MC-ICP-MS. ISMAS TRICON 2009, pp. 511–514.

Basu, A.R., Bandyopadhyay, P.K., Chakraborti, R., Zou, H., 2008. Large 3.4 Ga algoma type BIF in the eastern Indian craton. Geochimica et Cosmochimica Acta 72, A59.

Beall, A.P., Moresi, L., Cooper, C.M., 2018. Formation of cratonic lithosphere during the initiation of plate tectonics. Geology 46, 486–490.

Bell, E.A., Harrison, T.M., Issaku, E.K., Young, E.D., 2014. Eoarchean crustal evolution of the Jack Hills zircon source and loss of Hadean crust. Geochimica et Cosmochimica Acta 146, 27–42.

Belousova, E.A., Kostitsyn, Y.A., Griffin, W.L., Begg, G.C., O'Reilly, S.Y., Pearson, N.J., 2010. The growth of the continental crust: constraints from zircon Hf-isotope data. Lithos 119, 457–466.

Blichert-Toft, J., Albarède, F., 1997. The Lu–Hf isotope geochemistry of chondrites and the evolution of the mantle-crust system. Earth and Planetary Science Letters 148, 243–258.

Brown, M., 2008. Characteristic thermal regimes of plate tectonics and their metamorphic imprint throughout Earth history: when did Earth first adopt a plate tectonics mode of behavior?. In: Condie, K.C., Pease, V. (Eds.), When Did Plate Tectonics Begin on Planet Earth? Geological Society of America Special Paper, vol. 440, pp. 97–128.

Cavosie, A.J., Wilde, S.A., Liu, D.Y., Weiblen, P.W., John, W.V., 2004. International zoning and U–Th–Pb chemistry of Jack Hills detrital zircons: a mineral record of Early Archean to Mesoproterozoic (4348–1576 Ma) magmatism. Precambrian Research 135, 251–279.

Chattopadhyay, S., Upadhyay, D., Nanda, J.K., Mezger, K., Pruseth, K.L., Berndt, J., 2015. Proto-India was a part of rodinia: evidence from grenville-age suturing of the eastern Ghats province with the paleoarchean Singhbhum craton. Precambrian Research 266, 506–529.

Chaudhuri, T., Wan, Y., Mazumder, R., Ma, M., Dunyi Liu, D., 2018. Evidence of enriched, hadean mantle reservoir from 4.2-4.0 Ga zircon xenocrysts from paleoarchean TTGs of the Singhbhum craton, eastern India. Scientific Reports 8, 7069. https://doi.org/10.1038/s41598-018-25494-6.

Claoué-Long, J., Compston, W., Roberts, J., Fanning, C.M., 1995. Two Carboniferous ages: a comparison of SHRIMP zircon dating with conventional zircon ages and ^{40}Ar/^{39}Ar analysis. In: Berggren, W.A., Kent, D.V., Aubry, M.-P., Hardenbol, J. (Eds.), Geochronology, Time Scales, and Global Stratigraphic Correlation. Special Publications of SEPM, pp. 3–21.

Clements, B., Sevastjanova, I., Hall, R., Belousova, E.A., Griffin, W.L., Pearson, N., 2012. Detrital zircon U–Pb age and Hf-isotope perspective on sediment provenance and tectonic models in SE Asia. In: Rasbury, E.T., Hemming, S.R., Riggs, N.R. (Eds.), Mineralogical and Geochemical Approaches to Provenance, vol. 487. Geological Society of America Special Paper, pp. 37–61.

Collins, W.J., Belousova, E.A., Kemp, A.I., Murphy, J.B., 2011. Two contrasting Phanerozoic orogenic systems revealed by hafnium isotope data. Nature Geoscience 4, 333–337.

Condie, K.C., Aster, R.C., 2010. Episodic zircon age spectra of orogenic granitoids: the supercontinent connection and continental growth. Precambrian Research 180, 227–236.

Cumming, G.L., Richards, J.R., 1975. Ore lead isotopes in a continuously changing Earth. Earth and Planetary Science Letters 28, 155–171.

Dey, S., Topno, A., Liu, Y., Zong, K., 2017. Generation and evolution of Paleoarchean continental crust in the central part of the Singhbhum craton, eastern India. Precambrian Research 298, 268–291.

Dhuime, B., Hawkesworth, C.J., Cawood, P.A., Storey, C.D., 2012. A change in the geodynamics of continental growth 3 billion years ago. Science 335, 1334–1336.

Fisher, C.M., Vervoort, J.D., 2018. Using the magmatic record to constrain the growth of continental crust—The Eoarchean zircon Hf record of Greenland. Earth and Planetary Sciences 488, 79–91.

Frost, C.D., McLaughlin, J.F., Frost, B.R., Fanning, C.M., Swapp, S.M., Kruckenberg, S.C., Gonzalez, J., 2017. Hadean origins of Paleoarchean continental crust in the central Wyoming Province. The Geological Society of America Bulletin 129, 259–280.

Gerya, T.V., Stern, R.J., Baes, M., Sobolev, S.V., Whattam, S.A., 2015. Plate tectonics on the Earth triggered by plume-induced subduction initiation. Nature 527, 221–225.

Ghosh, S., De, S., Mukhopadhyay, J., 2016. Provenance of >2.8 Ga Keonjhar quartzite, Singhbhum craton, eastern India: implications for the nature of mesoarchean upper crust and geodynamics. The Journal of Geology 124, 331–351.

Greber, N.D., Dauphas, N., Bekker, A., Ptáček, M.P., Bindeman, I.N., Hoffman, A., 2017. Titanium isotopic evidence for felsic crust and plate tectonics 3.5 billion years ago. Science 357, 1271–1274.

Griffin, W.L., Belousova, E.A., O'Neill, C., O'Reilly, S.Y., Malkovets, V., Person, N.J., 2014. The world turns over: Hadean–Archean crust–mantle evolution. Lithos 189, 2–15.

Griffin, W.L., Belousova, E.A., Shee, S.R., Pearson, N.J., O'Reilly, S.Y., 2004. Archean crustal evolution in the northern Yilgarn Craton: U–Pb and Hf-isotope evidence from detrital zircons. Precambrian Research 131, 231–282.

Griffin, W.L., Belousova, E.A., Walters, S.G., O'Reilly, S.Y., 2006. Archean and proterozoic crustal evolution in the eastern succession of the Mt Isa district, Australia: U–Pb and Hf-isotope studies of detrital zircons. Australian Journal of Earth Sciences 53, 125–150.

Griffin, W.L., Pearson, N.J., Belousova, E.A., Jackson, S.R., van Achterbergh, E., O'Reilly, S.Y., Shee, S.R., 2000. The Hf isotope composition of cratonic mantle: LAM-MC-ICPMS analysis of zircon megacrysts in kimberlites. Geochimica et Cosmochimica Acta 64, 133–147.

Griffin, W.L., Pearson, N.J., Belousova, E.A., Saeed, A., 2007. Reply to "comment to short-communication 'comment: Hf-isotope heterogeneity in zircon 91500' by W. L. Griffin, N. J. Pearson, E. A. Belousova & A. Saeed (Chem. Geol. 233, (2006) 358–363)" by Corfu, F. Chemical Geology 244, 354–356.

Harrison, T.M., Bell, E.A., Boehnke, P., 2017. Hadean zircon petrochronology. Reviews in Mineralogy and Geochemistry 83 (1), 329–363.

Harrison, T.M., Schmitt, A.K., McCulloch, M.T., Lovera, O.M., 2008. Early (≥4.5 Ga) formation of terrestrial crust: Lu–Hf, δ^{18}O, and Ti thermometry results for Hadean zircons. Earth and Planetary Science Letters 268, 476–486.

Hawkesworth, C.J., Cawood, P.A., Dhuime, B., Kemp, A.I.S., 2017. Earth's continental lithosphere through time. Annual Reviews of Earth and Planetary Sciences 45, 169–198.

Hiess, J., Bennett, V.C., Nutman, A.P., Williams, I.S., 2009. In situ U–Pb, O and Hf isotopic compositions of zircon and olivine from Eoarchean rocks, West Greenland: new insights into making old crust. Geochimica et Cosmochimica Acta 73, 4489–4516.

Iizuka, T., Komiya, T., Johnson, S.P., Kon, Y., Maruyama, S., Hirata, T., 2009. Reworking of Hadean crust in the Acasta gneisses, north western Canada: evidence from in situ Lu–Hf isotope analysis of zircon. Chemical Geology 259, 230–239.

Iizuka, T., Yamaguchi, T., Itano, K., Hibiya, R., Suzuki, K., 2017. What Hf isotopes in zircon tell us about crust–mantle evolution. Lithos 274–275, 304–327.

Jackson, S.E., Pearson, N.J., Griffin, W.L., Belousova, E.A., 2004. The application of laser ablation-inductively coupled plasma-mass spectrometry to in situ U–Pb zircon geochronology. Chemical Geology 211, 47–69.

Johnson, T.E., Brown, M., Gardiner, N.J., Kirkland, C.L., Smithies, R.H., 2017. Earth's first stable continents did not form by subduction. Nature 543, 239–242.

Kaur, P., Zeh, A., Chaudhri, N., 2014. Characterisation and U–Pb–Hf isotope record of the 3.55 felsic crust from the Bundelkhand Craton, northern India. Precambrian Research 255, 236–244.

Kemp, A.I.S., Hickman, A.H., Kirkland, C.L., Vervoort, J.D., 2015. Hf isotopes in detrital and inherited zircons of the Pilbara Craton provide no evidence for Hadean continents. Precambrian Research 261, 112–126.

Kemp, A.I.S., Wilde, S.A., Hawkesworth, C.J., Coath, C.D., Nemchin, A., Pidgeon, R.T., Vervoort, J.D., DuFrane, S.A., 2010. Hadean crustal evolution revisited: new constraints from Pb–Hf isotope systematics of the Jack Hills zircons. Earth and Planetary Science Letters 296, 45–56.

Korenaga, J., 2013. Initiation and evolution of plate tectonics on Earth: Theories and observations. Annual Review of Earth and Planetary Sciences 41, 117–151.

Ludwig, K.R., 2003. Mathematical-statistical treatment of data and errors for ^{230}Th/U geochronology, Uranium-series geochemistry. Reviews in Mineralogy and Geochemistry 52, 631–656.

Martin, H., Moyen, J.-F., Guitreau, M., Blichert-Toft, J., Pennec, J.-L., 2014. Why Archaean TTG cannot be generated by MORB melting in subduction zones. Lithos 198–199, 1–13.

Miller, S.R., Mueller, P.A., Meert, J.G., Kamenov, G.D., Pivarunas, A.F., Sinha, A.K., Pandit, M.K., 2018. Detrital zircons reveal evidence of hadean crust in the Singhbhum craton, India. The Journal of Geology 126, 541–552.

Misra, S., Deomurari, M.P., Wiedenbeck, M., Goswami, J.N., Ray, S., Saha, A.K., 1999. ^{207}Pb/^{206}Pb zircon ages and the evolution of the Singhbhum craton, eastern India: an ion microprobe study. Precambrian Research 93, 139–151.

Mondal, S.K., Frei, R., Ripley, E.M., 2007. Os isotope systematics of mesoarchean chromitite-PGE deposits in the Singhbhum Craton (India): implications for the evolution of lithospheric mantle. Chemical Geology 244, 391–408.

Mueller, P.A., Nutman, A.P., 2017. The Archean-Hadean Earth: modern paradigms and ancient processes. The Web of Geological Sciences Advances Impacts and Interactions II 523, 75–237.

Mueller, P.A., Wooden, J.L., 2012. Trace element and Lu-Hf systematics in hadean-archean detrital zircons: implications for crustal evolution. The Journal of Geology 120, 15–29.

Mukhopadhyay, D., 2001. The Archean nucleus of Singhbhum: the present state of knowledge. Gondwana Research 4, 307–318.

Mukhopadhyay, J., Beukes, N.J., Armstrong, R.A., Zimmermann, U., Ghosh, G., Medda, R.A., 2008. Dating the oldest greenstone in India: a 3.51-Ga precise U-Pb

SHRIMP zircon age for dacitic lava of the Southern Iron Ore Group, Singhbhum craton. The Journal of Geology 116, 449–461.
Mukhopadhyay, J., Crowley, Q.G., Ghosh, S., Ghosh, G., Chakrabarti, K., Misra, B., Heron, K., Bose, S., 2014. Oxygenation of the archean atmosphere: new paleosol constraints from eastern India. Geology 42, 923–926.
Mukhopadhyay, J., Ghosh, G., Zimmermann, U., Guha, S., Mukherjee, T., 2012. 3.51 Ga bimodal volcanics-BIF-ultramafic succession from Singhbhum craton: implications for Paleoarchean geodynamic processes from the oldest greenstone succession of Indian Subcontinent. Geological Journal 47, 284–311.
Næraa, T., Schersten, A., Rosing, M.T., Kemp, A.I.S., Hoffmann, J.E., Kokfelt, T.F., Whitehouse, M.J., 2012. Hafnium isotope evidence for a transition in the dynamics of continental growth 3.2 Gyr ago. Nature 485, 627–630.
Naqvi, S.M., 2005. Geology and Evolution of the Indian Plate (From Hadean to Holocene: 4 Ga to 4 Ka). Capital Publishing, New Delhi, p. 450.
Nelson, D., Bhattacharya, H.N., Thern, E.R., Altermann, W., 2014. Geochemical and ion-microprobe U-Pb zircon constraints on the Archean evolution of Singhbhum Craton, eastern India. Precambrian Research 255, 412–432.
Nowell, G.M., Kempton, P.D., Noble, S.R., Fitton, J.G., Saunders, A.D., Mahoney, J.J., Taylor, R.N., 1998. High precision Hf isotopic measurements of MORB and OIB by thermal ionization mass spectrometry: insights into the depleted mantle. Chemical Geology 149, 211–233.
Nutman, A.P., Bennett, V.C., Friend, C.L., Hidaka, H., Yi, K., Lee, S.R., Kamiichi, T., 2013. The Itsaq gneiss Complex of Greenland: episodic 3900 to 3660 juvenile crust formation and recycling in the 3660 to 3600 Ma Isukasian Orogeny. American Journal of Science 313, 877–911.
Nutman, A.P., Bennett, V.C., Friend, C.R.L., 2015. Proposal for a continent 'Istaquia' amalgamated at 3.66 Ga and rifted apart from 3.53 Ga: initiation of a Wilson cycle near the start of the rock record. American Journal of Science 315, 509–536.
O'Neill, C., Debaille, V., 2014. The evolution of Hadean-Eoarchean geodynamics. Earth and Planetary Science Letters 406, 49–58.
Prabhakar, N., Bhattacharya, A., 2013. Paleoarchean thrust-and-fold belt tectonics in the Singhbhum craton, eastern India. Precambrian Research 231, 106–121.
Ramakrishnan, M., Vaidyanathan, R., 2008. Geology of India. Journal Geological Society of India, Bangalore, p. 556.
Roberts, N.M.W., Spencer, C.J., 2015. The zircon archive of continent formation through time. In: Roberts, N.M.W., Van Kranendonk, M., Parman, S., Shirey, S., Clift, P.D. (Eds.), Continent Formation through Time, vol. 389. Geological Society of London, Special Publications, pp. 197–225.
Roy, A.B., Bhattacharya, H.N., 2012. Tectonostratigraphic and geochronologic reappraisal constraining the growth and evolution of Singhbhum Archean craton, eastern India. Journal of the Geological Society of India 80, 455–469.
Rubatto, D., 2002. Zircon trace element geochemistry: partitioning with garnet and the link between U-Pb ages and metamorphism. Chemical Geology 184, 123–138.
Saha, A.K., Ray, S.L., Sarkar, S.N., 1988. Early history of the Earth: evidence from the eastern Indian shield. In: Mukhopadhyay, D. (Ed.), Precambrian of the Eastern Indian Shield, vol. 8. Geological Society of India, Memoir, pp. 13–37.
Sandiford, M., Kranendonk, M.J.V., Bodorkos, S., 2004. Conductive incubation and the origin of dome-and-keel structure in Archaean granite-greenstone terrains: a model based on the eastern Pilbara Craton, Western Australia. Tectonics 23, TC1009.
Sarkar, S.C., Gupta, A., 2012. Crustal Evolution and Metallogeny in India. Cambridge University Press, Cambridge, p. 840.
Sarkar, S.N., Saha, A.K., 1983. Structure and Tectonics of the Singhbhum – Orissa Iron Ore Craton, Eastern India. Recent Research Geology (Structure and Tectonics of the Precambrian Rocks), vol. 10. Hindusthan Pub Corp., Delhi, India, pp. 1–25.
Satkoski, A.M., Bickford, M.E., Samson, S.D., Bauer, R.L., Mueller, P.A., Kamenov, G.D., 2013. Geochemical and Hf–Nd isotopic constraints on the crustal evolution of Archean rocks from the Minnesota River Valley, USA. Precambrian Research 224, 36–50.
Scherer, E., Munker, C., Mezger, K., 2001. Calibration of the Lutetium-hafnium clock. Science 293, 683–687.
Smithies, R.H., Champion, D.C., Van Kranendonk, M.J., 2009. Formation of Paleoarchean continental crust through infracrustal melting of enriched basalt. Earth and Planetary Science Letters 281, 298–306.
Spencer, C.J., Hawkesworth, C.J., Cawood, P.A., Dhuime, B., 2013. Not all supercontinents are created equal: gondwana-Rodinia case study. Geology 41, 795–798.
Stern, R.J., 2005. Evidence from ophiolites, blueschists, and ultrahigh-pressure metamorphic terranes that the modern episode of subduction tectonics began in neoproterozoic time. Geology 33, 557–560.
Stern, R.A., Bodorkos, S., Kamo, S.L., Hickman, A.H., Corfu, F., 2009. Measurement of SIMS instrumental mass fractionation of Pb isotopes during zircon Dating. Geostandards and Geoanalytical Research 33, 145–168.
Tait, J., Zimmermann, U., Miyazaki, T., Presnyakov, S., Chang, Q., Mukhopadhyay, J., Sergeev, S., 2011. Possible juvenile Paleoarchean TTG magmatism in eastern India and its constraints for the evolution of the Singhbhum craton. Geological Magazine 148, 340–347.
Tang, M., Chen, K., Rudnick, R.L., 2016. Archean upper crust transition from mafic to felsic marks the onset of plate tectonics. Science 351, 372–375.
Upadhyay, D., Chattopadhyay, S., Kooijman, E., Mezger, K., Berndt, J., 2014. Magmatic and metamorphic history of Paleoarchean tonalite-trondhjemite-granodiorite (TTG) suite from the Singhbhum craton, eastern India. Precambrian Research 252, 180–190.
Vermeesch, P., 2018. IsoplotR: a free and open toolbox for geochronology. Geoscience Frontiers 9, 1479–1493.
Vijaya Kumar, T., Bhaskar Rao, Y.J., Plavsa, D., Collins, A.S., Tomson, J.K., Vijaya Gopal, B., Babu, E.V.S.S.K., 2017. Zircon U-Pb ages and Hf isotopic systematics of charnockite gneisses from the Ediacaran-Cambrian high-grade metamorphic terrains, southern India: constraints on crust formation, recycling and Gondwana correlations. The Geological Society of America Bulletin 129, 625–648.
Voice, P.J., Kowalewski, M., Eriksson, K.A., 2011. Quantifying the timing and rate of crustal evolution: global compilation of radiometrically dated detrital zircon grains. The Journal of Geology 119, 109–126.
Wan, Y.-S., Liu, D.-Y., Dong, C.-Y., Xie, H.-Q., Kröner, A., Ma, M.-Z., Liu, S.-J., Xie, S.-W., Ren, P., 2015. Formation and evolution of Archean continental crust of the North China craton. In: Zhai, M. (Ed.), Precambrian Geology of China. Springer-Verlag, pp. 59–135.
Wiemer, D., Schrank, C.E., Murphy, D.T., Wenham, L., Allen, C.M., 2018. Earth's oldest stable crust in the Pilbara Craton formed by cyclic gravitational overturns. Nature Geoscience 11, 357–361.
Wilde, S.A., Valley, J.W., Peck, W.H., Graham, C.M., 2001. Evidence from detrital zircons for the existence of continental crust and oceans on the Earth 4.4 Gyr ago. Nature 409, 175–178.
Williams, I.S., 1998. U–Th–Pb geochronology by ion microprobe. In: McKibben, M.A., Shanks III, W.C., Ridley, W.I. (Eds.), Applications of Microanalytical Techniques to Understanding Mineralizing Processes. Reviews in Economic Geology, vol. 7, pp. 1–35.
Williams, I.S., Claesson, S., 1987. Isotopic evidence for the Precambrian provenance and Caledonian metamorphism of high grade paragneisses from the Seve Nappes, Scandinavian Caledonides. II. Ion microprobe zircon U-Th-Pb. Contributions to Mineralogy and Petrology 97, 205–217.
Wu, F.-Y., Zhang, Y.-B., Yang, J.-H., Xie, L.-W., Yang, Y.-H., 2008. Zircon U–Pb and Hf isotopic constraints on the early archean crustal evolution in anshan of the north China craton. Precambrian Research 167, 339–362.
Zeh, A., Gerdes, A., Barton Jr., J.M., Klemd, R., 2010. U–Th–Pb and Lu–Hf systematics of zircon from TTG's, leucosomes, anorthosites and quartzites of the Limpopo Belt (South Africa): constraints for the formation, recycling, and metamorphism of Paleoarchean crust. Precambrian Research 179, 50–68.
Zeh, A., Gerdes, A., Heubeck, C., 2013. U-Pb and Hf isotope data from detrital zircons of the Barberton greenstone belt: constraints on provenance and Archean crustal evolution. Geological Society of London 170, 215–223.
Zeh, A., Gerdes, A., Millonig, L., 2011. Hafnium isotope record of the Ancient Gneiss Complex, Swaziland, southern Africa: evidence for Archean crust–mantle formation and crust reworking between 3.66 and 2.73 Gyr. Geological Society of London 168, 953–963.
Zeh, A., Stern, R., Gerdes, A., 2014. The oldest zircons of Africa—their U–Pb–Hf–O isotope and trace element systematics, and implications for Hadean to Archean crust–mantle evolution. Precambrian Research 241, 203–230.